ACI STRUCTURAL JOURNAL TECHNICAL PAPER

Title no. 107-S59

Shear Behavior of Steel Fiber-Reinforced Concrete Beams without Stirrup Reinforcement

by Hai H. Dinh, Gustavo J. Parra-Montesinos, and James K. Wight

Results from a comprehensive investigation aimed at studying the behavior of steel fiber-reinforced concrete (SFRC) beams in shear, as well as the possibility of using steel fibers as minimum shear reinforcement, are presented. A total of 28 simply supported beams with a shear span-to-effective depth ratio of approximately 3.5 were subjected to a monotonically increased, concentrated load. The target concrete compressive strength for all of the beams was 41 MPa (6000 psi). The studied parameters included beam depth (455 or 685 mm [18 or 27 in.]), fiber length (30 or 60 mm [1.2 or 2.4 in.]), fiber aspect ratio (55 or 80), fiber strength (1100 or 2300 MPa [160 or 330 ksi]), and fiber volume fraction (between 0.75 and 1.5%). In total, three types of steel fibers were considered, all with hooks at their ends. The behavior of beams failing in shear prior to or after flexural yielding was also investigated by varying the longitudinal reinforcement ratio (1.6, 2.0, and 2.7%).

Test results showed that the use of hooked steel fibers in a volume fraction greater than or equal to 0.75% led to multiple diagonal cracking and a substantial increase in shear strength compared to reinforced concrete (RC) beams without stirrup reinforcement. All SFRC beams sustained a peak shear stress of at least $0.33\sqrt{f'_c}$ MPa ($4.0\sqrt{f'_c}$ psi). The results also indicated that the hooked steel fibers evaluated in this investigation can safely be used as minimum shear reinforcement in RC beams constructed with normal-strength concrete and within the range of member depths considered.

Keywords: ductility; fiber-reinforced concrete; hooked steel fibers; shear strength; stirrups.

INTRODUCTION

The use of discontinuous, randomly oriented fibers has long been recognized to provide post-cracking tensile resistance to concrete. Thus, their use as shear reinforcement in reinforced concrete (RC) beams has been the focus of several investigations in the past four decades (an extensive list of references was reported by Parra-Montesinos [2006]). Fiber reinforcement enhances shear resistance by transferring tensile stresses across diagonal cracks and reducing diagonal crack spacing and width, which increases aggregate interlock. The reduction in crack spacing due to the presence of fibers indicates that the use of fiber reinforcement could potentially lead to a reduction or even an elimination of the shear size effect in beams without stirrup reinforcement, whose shear strength is known to decrease as the overall beam depth increases (Wight and MacGregor 2008). The effectiveness of fiber reinforcement to increase shear resistance, however, is dependent on several factors, including fiber properties (that is, material properties, aspect ratio, and shape), fiber content, and bond stress versus slip response of fibers.

A survey of published experimental data conducted by Parra-Montesinos (2006) revealed that an average shear stress of $0.3\sqrt{f'_c}$ MPa ($3.6\sqrt{f'_c}$ psi) represented a lower bound for the shear strength of beams with deformed steel fibers in volume fractions V_f greater than or equal to 0.75%. Most of the available data, however, corresponded to beams with overall depths smaller than 405 mm (16 in.). These data were used as the basis for a new provision in the 2008 ACI Building Code (ACI Committee 318 2008), which allows the use of deformed steel fibers in volume fractions greater than or equal to 0.75% as minimum shear reinforcement in normal-strength concrete beams subjected to factored shear stresses between $\phi(1/12)\sqrt{f'_c}$ and $\phi(1/6)\sqrt{f'_c}$ MPa ($\phi\, 1\sqrt{f'_c}$ and $\phi 2\sqrt{f'_c}$ psi) and with an overall depth not exceeding 610 mm (24 in.). Besides the minimum fiber volume fraction of 0.75%, the ACI Code prescribes a flexural performance criteria for the acceptance of steel fiber-reinforced concrete (SFRC) as a replacement for minimum shear reinforcement, based on ASTM C1609 (2005) four-point bending tests.

The research presented herein was aimed at experimentally investigating the behavior of relatively large SFRC beams in shear, which is not well known due to the limited availability of test data. In particular, this research focused on the study of: 1) the behavior and shear strength of SFRC beams with various depths and reinforcement ratios; 2) the effect of fiber volume fraction, aspect ratio, and strength on the shear behavior of SFRC beams; and 3) the possibility of using steel fibers as minimum shear reinforcement in RC beams.

RESEARCH SIGNIFICANCE

Results from a large experimental program aimed at evaluating the shear behavior of SFRC beams are presented. Data presented herein are considered unique in the sense that they provide information on the effect of parameters such as fiber geometry, strength and volume fraction, and longitudinal reinforcement ratio on the shear behavior of relatively large SFRC beams.

EXPERIMENTAL PROGRAM

A total of 28 beams were tested under a monotonically increased concentrated load to investigate the shear behavior of SFRC beams. The experimental program consisted of two series of beams: Series B18, with an overall beam depth of 455 mm (18 in.), and Series B27, with a beam depth of 685 mm (27 in.). There were eight pairs of beams for Series B18 and four pairs plus four single beams for Series B27. Beams from each pair were nominally "identical" to reduce the uncertainty of the shear data. Table 1 lists the properties of the test beams. For Series B18, a pair of beams with neither

ACI Structural Journal, V. 107, No. 5, September-October 2010.
MS No. S-2009-277.R1 received December 16, 2009, and reviewed under Institute publication policies. Pertinent discussion including author's closure, if any, will be published in the July-August 2011 *ACI Structural Journal* if the discussion is received by March 1, 2011.

Hai H. Dinh *is an Engineer at Moffatt and Nichol, working on the San Francisco Oakland Bay Bridge East Span Seismic Safety Project. He received his PhD from the University of Michigan, Ann Arbor, MI, in 2009. His research interests include fiber-reinforced concrete.*

Gustavo J. Parra-Montesinos *is an Associate Professor in the Department of Civil and Environmental Engineering at the University of Michigan. He is Chair of ACI Committee 335, Composite and Hybrid Structures, a member of the ACI Publications Committee, and a member of ACI Committees 318, Structural Concrete Building Code; 318-D, Flexure and Axial Loads: Beams, Slabs, and Columns; and 318-R, Code Reorganization; and Joint ACI-ASCE Committee 352, Joints and Connections in Monolithic Concrete Structures. His research interests include the behavior and design of reinforced concrete, fiber-reinforced concrete, and composite steel-concrete structures.*

James K. Wight *is the Frank E. Richart Jr. Collegiate Professor of Civil Engineering at the University of Michigan. He is Past Chair of ACI Committee 318, Structural Concrete Building Code, and Joint ACI-ASCE Committee 352, Joints and Connections in Monolithic Concrete Structures.*

fiber nor stirrup reinforcement was tested (B18-0) to compare the behavior of regular concrete beams with that of the SFRC beams. For Series B27, one beam with regular concrete and no stirrup reinforcement was tested (Beam B27-7). A second regular concrete beam with stirrup reinforcement satisfying the minimum requirement in the ACI Code (ACI Committee 318 2008) was also tested (Beam B27-8) to compare the behavior of SFRC beams with that of beams with minimum stirrup reinforcement. Detailed information about this testing program can be found elsewhere (Dinh 2009).

Details of test beams

Figures 1 and 2 show the overall geometry and reinforcement detailing for beams in Series B18 and B27, respectively. Each beam was designed to fail in the longer shear span, with a span-to-effective depth (a/d) ratio of approximately 3.5 that was selected to reduce any significant contribution from arch action to beam shear strength. The shorter span was reinforced with sufficient stirrup reinforcement to prevent any significant shear distress during testing. All of the beams were constructed with regular-strength concrete with a target compressive strength of 41 MPa (6000 psi).

Three types of steel fibers, all with hooked ends, were evaluated in volume fractions of either 0.75%, or 1% or 1.5%. Fiber Types 1 and 3 were 30 mm (1.2 in.) long with an aspect (length-to-diameter) ratio of 55 and 80, respectively. Type 2 fibers were 60 mm (2.4 in.) long with an aspect ratio

Table 1—Beam properties and summary of test results

Beam	d, mm	a/d	ρ, %	Fiber type	V_f, %	f'_c, MPa	P_u, kN	v_u, MPa	$v_u/\sqrt{f'_c}$	Failure mode
B18-0a	381	3.43	2.7	—	—	42.8	168	1.1	0.17	DT
B18-0b	381	3.43	2.7	—	—	42.8	162	1.1	0.17	DT
B18-1a	381	3.43	2.0	1	0.75	44.8	441	2.9	0.44	SC+ST*
B18-1b	381	3.43	2.0	1	0.75	44.8	413	2.8	0.41	ST+DT*
B18-2a	381	3.50	2.0	1	1.00	38.1	437	3.0	0.49	ST+DT*
B18-2b	381	3.50	2.0	1	1.00	38.1	445	3.1	0.50	ST+DT*
B18-2c	381	3.50	2.7	1	1.00	38.1	503	3.5	0.57	NA*
B18-2d	381	3.50	2.7	1	1.00	38.1	367	2.6	0.41	NA†
B18-3a	381	3.43	2.7	1	1.50	31.0	384	2.6	0.46	ST+DT†
B18-3b	381	3.43	2.7	1	1.50	31.0	507	3.4	0.61	SC+ST
B18-3c	381	3.43	2.7	1	1.50	44.9	494	3.3	0.49	ST+DT
B18-3d	381	3.43	2.7	1	1.50	44.9	490	3.3	0.49	ST+DT
B18-5a	610	3.43	2.7	2	1.00	49.2	445	3.0	0.43	DT
B18-5b	610	3.43	2.7	2	1.00	49.2	565	3.8	0.54	ST+DT
B18-7a	610	3.43	2.0	3	0.75	43.3	498	3.3	0.50	ST+DT*
B18-7b	610	3.43	2.0	3	0.75	43.3	490	3.3	0.50	ST+DT*
B27-1a	610	3.50	2.0	1	0.75	50.8	908	2.9	0.41	ST+DT
B27-1b	610	3.50	2.0	1	0.75	50.8	837	2.7	0.38	DT
B27-2a	610	3.50	2.0	2	0.75	28.7	872	2.8	0.53	SC+ST
B27-2b	610	3.50	2.0	2	0.75	28.7	854	2.8	0.52	DT
B27-3a	610	3.50	1.6	1	0.75	42.3	846	2.7	0.42	F*
B27-3b	610	3.50	1.6	1	0.75	42.3	863	2.8	0.43	SC+ST*
B27-4a	610	3.50	1.6	2	0.75	29.6	663	2.1	0.40	ST+DT†
B27-4b	610	3.50	1.6	2	0.75	29.6	556	1.8	0.33	ST+DT†
B27-5	610	3.50	2.1	1	1.50	44.4	1081	3.5	0.53	SC+ST*
B27-6	610	3.50	2.1	2	1.50	42.8	1046	3.4	0.52	ST+DT*
B27-7	610	3.50	1.6	—	—	37.0	402	1.3	0.21	DT
B27-8‡	610	3.50	1.6	—	—‡	37.0	570	1.8	0.30	DT

*Reinforcement yielded.

†Significant bond degradation near support.

‡Beam contained minimum shear reinforcement (refer to Fig. 2 for reinforcement details).

Note: Width of beams in Series B18 and B27 is 152 and 203 mm (6 and 8 in.), respectively; d is beam effective depth; a is shear span; ρ is tension reinforcement ratio; V_f is fiber volume fraction; f'_c is concrete cylinder strength; P_u is peak load; v_u is peak average shear stress; DT is diagonal tension; SC is shear compression; ST is shear tension; F is flexure; NA is not available; 1 mm = 0.0394 in.; 1 kN = 0.225 kips; and 1 MPa = 145 psi.

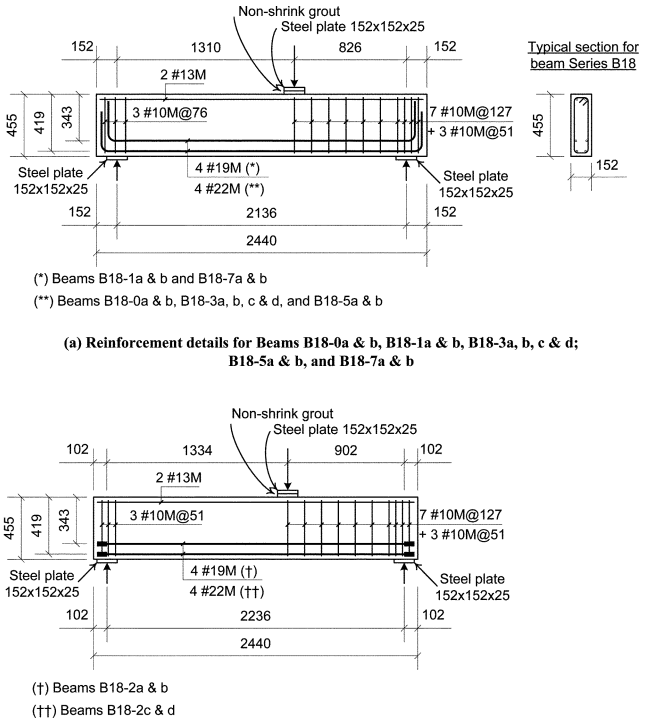

(a) Reinforcement details for Beams B18-0a & b, B18-1a & b, B18-3a, b, c & d; B18-5a & b, and B18-7a & b

Notes: (1) all dimensions are in mm; 1 mm = 0.0394 in.

(2) bars #10M, 13M, 19M, and 22M have an area of 71, 129, 284, and 387 mm^2, respectively

(b) Reinforcement details for Beams B18-2a, b, c & d

Fig. 1—Geometry and reinforcement details for beams in Series B18. (Note: 1 mm^2 = 0.0015 in.^{2})

of 80. Figure 3 shows a photo of fiber Types 1 and 2. Fiber Types 1 and 2 can be considered to be regular-strength fibers (with a tensile strength of approximately 1100 MPa [160 ksi]), whereas the Type 3 fiber was made of a high-strength wire (with a tensile strength of 2300 MPa [330 ksi]).

Another aspect investigated was the longitudinal reinforcement ratio ρ, calculated as the area of tension steel A_s divided by the product between the beam width b and the effective depth d. Longitudinal reinforcement affects beam shear strength by influencing the size of the compression zone and by providing shear resistance through dowel action. Moreover, depending on the amount of steel reinforcement used, flexural yielding might develop first, followed by shear failure of the beam. This is particularly important for cases in which a shear failure develops after limited flexural yielding has occurred; and, thus, the beam ductility is not considered to be acceptable. Beams with three different reinforcement ratios were tested (ρ of approximately 1.6, 2.0, and 2.7%) to evaluate the behavior of beams failing in shear prior to or after flexural yielding.

Instrumentation

Strains in the beam longitudinal reinforcement were measured through strain gauges placed at various locations. In addition to strain gauges, two linear potentiometers were installed under the loading point of each beam to measure its deflection. The strain field in the critical shear span of the test beams was monitored through an active infrared optical position tracking system (Northern Digital Inc. 2005).

Concrete casting

Concrete was either provided by a local ready mix concrete supplier or mixed in the Structural Engineering

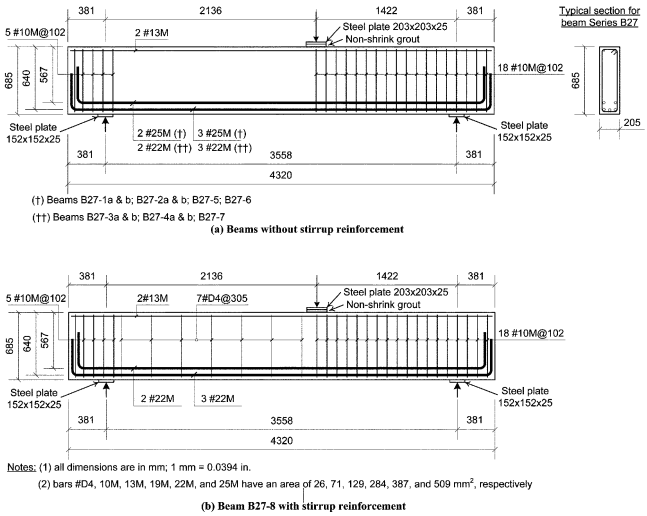

(a) Beams without stirrup reinforcement

Notes: (1) all dimensions are in mm; 1 mm = 0.0394 in.

(2) bars #D4, 10M, 13M, 19M, 22M, and 25M have an area of 26, 71, 129, 284, 387, and 509 mm^2, respectively

(b) Beam B27-8 with stirrup reinforcement

Fig. 2—Geometry and reinforcement details for beams in Series B27. (Note: 1 mm^2 = 0.0015 in.^{2})

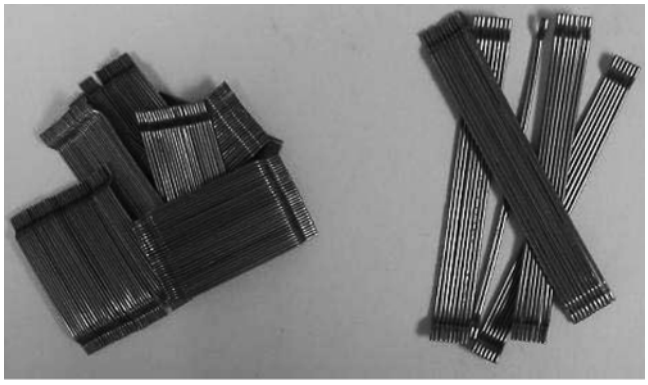

Fig. 3—Hooked steel fibers.

Laboratory at the University of Michigan. In all cases, crushed limestone with 10 mm (3/8 in.) maximum size was used. Fiber reinforcement was added last to the concrete and mixed for a few minutes until a uniform distribution of fibers could be seen. In the case of ready mix concrete, fibers were added to the concrete on site.

Even though good workability was obtained for all mixtures, fiber congestion was observed along the flexural reinforcement if the clear spacing between reinforcing bars was substantially less than the fiber length. Fiber congestion was therefore more pronounced for concrete mixed with longer fibers (60 mm [2.4 in.] in length). This led to voids in the critical shear span of four of the beams, which were subsequently repaired by pouring high-strength grout into the voids. This limited experience suggests that minimum clear spacing between bars should not be less than the fiber length to prevent lumping of fibers along the longitudinal reinforcement. After casting, all beam specimens were moist-cured and covered with plastic sheets. Beams were demolded at the age of 7 days and air cured in the laboratory until being tested.

MATERIAL PROPERTIES

Fiber-reinforced concrete

The compressive strength of the SFRC was determined through compression tests of 100 x 200 mm (4 x 8 in.) cylinders. Measured compressive strengths are listed in Table 1.

The flexural behavior of the SFRCs was evaluated through ASTM C1609 (2005) four-point bending tests on 150 x 150 x 510 mm (6 x 6 x 20 in.) beams (455 mm [18 in.] span). Each test was carried up to a midspan deflection of 1/150 of the span length (3 mm [0.12 in.]). Detailed information about these ASTM C1609 tests can be found elsewhere (Dinh 2009). Representative responses for SFRCs with 0.75 and 1.5% fiber volume fraction are shown in Fig. 4. These responses represent the average of three or more individual tests, except for Beam B27-5, for which only two beams were tested. As can be seen, the SFRCs with short (30 mm long [1.18 in.]), regular-strength fibers (Type 1) in a 0.75% volume fraction exhibited a deflection-softening response with a residual strength at the end of the test less than 50% of the first cracking strength. Doubling the amount of Type 1 fibers to 1.5% by volume allowed the SFRC to maintain most of its flexural cracking strength up to a midspan deflection of approximately 1/600 of the span length (0.75 mm [0.04 in.]), but as the deflection increased, the flexural strength decayed to a residual value at the end of the test slightly greater than 50% of the first cracking strength. The use of high-strength hooked fibers (Type 3) in a 0.75% volume fraction led to a short hardening response and an increased residual strength compared to the SFRC with regular-strength (Type 1) fibers. This is attributed to the greater plastic strength of the fiber hooks, as well as the increased fiber aspect ratio.

The SFRCs with 60 mm (2.4 in.) long, regular-strength fibers (Type 2) exhibited a more ductile response compared to that of the SFRCs with shorter fibers, regardless of the fiber content. This is not surprising, given the ability of the longer fibers to more effectively bridge cracks with larger widths.

Table 2—Reinforcing bar properties

Bar size	f_y, MPa (ksi)	ε_{sh}	f_{su}, MPa (ksi)
D4*	627 (91)†	—†	661 (96)
10M	414 (60)	—‡	579 (84)
13M	461 (67)	0.0080	689 (100)
19M	496 (72)	0.0090	751 (109)
22M	448 (65)	0.0080	675 (98)
25M	455 (66)	0.0080	689 (100)

*Area is 25.8 mm^2 (0.04 in.^{2}).
†No clear yield point (calculated based on 0.2% strain offset).
‡Strain hardening initiated as soon as steel yielded.

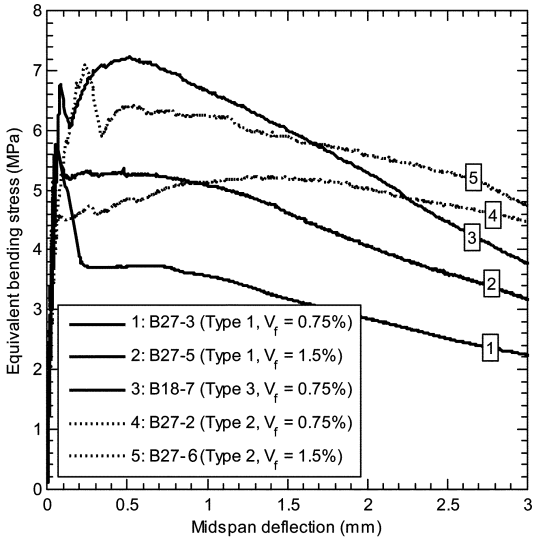

Fig. 4—Equivalent bending stress versus midspan deflection relationship from four-point bending tests.

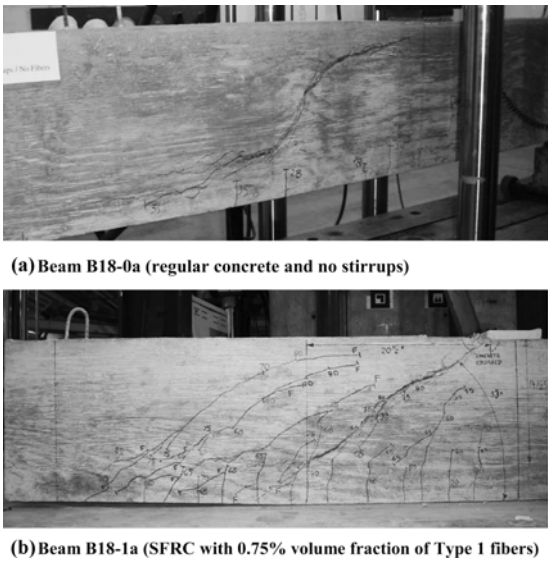

Fig. 5—Cracking pattern in RC versus SFRC beams.

Steel reinforcing bars

Direct tensile tests on reinforcing bar samples were conducted to evaluate the stress versus strain response of the steel reinforcement. Yield strength and strain, strain at initiation of strain hardening, and ultimate strength data are listed in Table 2.

OVERALL BEHAVIOR OF TEST BEAMS

The overall behavior of the test beams was evaluated based on their crack distribution, average shear stress (load) versus displacement response, ultimate strength, failure mode, and strain field in the critical shear span.

Crack distribution and average shear stress versus displacement response

The crack patterns for the RC and SFRC beams were distinctly different. While the RC beams without transverse reinforcement exhibited a single inclined crack followed by a brittle shear failure (Fig. 5(a)), all SFRC beams showed at least two diagonal cracks (Fig. 5(b)). With a minimum amount of stirrup reinforcement, a minor improvement in cracking pattern was observed for Beam B27-8 compared to the RC beam without stirrups. It is worth mentioning that while multiple diagonal cracking occurred in all SFRC beams, the spacing between diagonal cracks was larger for beams with a larger effective depth. The average horizontal spacing between cracks, however, was approximately 0.4d, regardless of the beam depth.

Figure 6 shows the average shear stress versus displacement response for all test beams. The shape of the shear stress versus displacement response of the SFRC test beams differed depending on the amount of longitudinal reinforcement provided, which dictated whether a shear failure occurred prior to or after flexural yielding. Beams that exhibited flexural yielding are identified in Table 1. For beams that failed in

shear prior to flexural yielding, the shear stress versus displacement response was characterized by a nearly linear response up to failure (for example, Beams B18-2c and d). The presence of fibers, however, allowed the development of multiple diagonal cracks and the widening of at least one of them prior to a shear failure, which provided some warning about the imminence of failure. Even for these beams the failure was rather sudden. For cases in which flexural yielding preceded a shear failure, the shear stress versus displacement response exhibited a well-defined yield plateau (refer to Beams B18-2a and b). Because the shear force demand associated with flexural yielding was close to the beam shear capacity when behaving in the elastic range (prior to flexural yielding), however, the degree of yielding often varied, even within the same pair of beams.

The behavior of the RC beams with or without stirrups (Beams B18-0a and b, B27-7, and B27-8) was brittle. For the control beams without stirrup reinforcement, the shear stress at failure was substantially lower than that for the SFRC beams. Although the addition of stirrup reinforcement (30% greater than the minimum required in the 2008 ACI Code) led to a 40% increase in shear strength, the shear stress versus displacement response was still nearly linear up to failure.

Failure modes

The failure mode for each test beam is listed in Table 1. All test beams ultimately failed in shear, except for Beam B27-3a, which exhibited a flexural failure characterized by crushing of the beam compression zone near the load point after substantial yielding of the longitudinal tension reinforcement had taken place.

Three types of shear failures were observed: 1) diagonal tension; 2) a combination of diagonal tension and shear-tension; and 3) a combination of shear-compression and shear-tension. For a diagonal tension failure, the opening of the critical inclined crack occurred in the beam middepth region and propagated toward both the reinforcement level and the compression region. At failure, the critical crack extended through the beam compression zone without causing crushing of the concrete. When combined with a shear-tension failure, the critical diagonal crack propagated along the longitudinal reinforcement toward the support.

For the failure mode that was considered a combination of shear-compression and shear-tension failures, the widening of the critical crack started at the reinforcement level and extended up, toward the loading point. Beam failure was triggered by the crushing of the concrete in the beam compression zone adjacent to the loading point, accompanied by a significant splitting along the top layer of longitudinal tension reinforcement.

Of all beam specimens, four exhibited a shear failure believed to have been triggered by significant deterioration of bond along the longitudinal reinforcement near the support region (refer to Table 1). This bond deterioration was identified through strain gauge readings and was

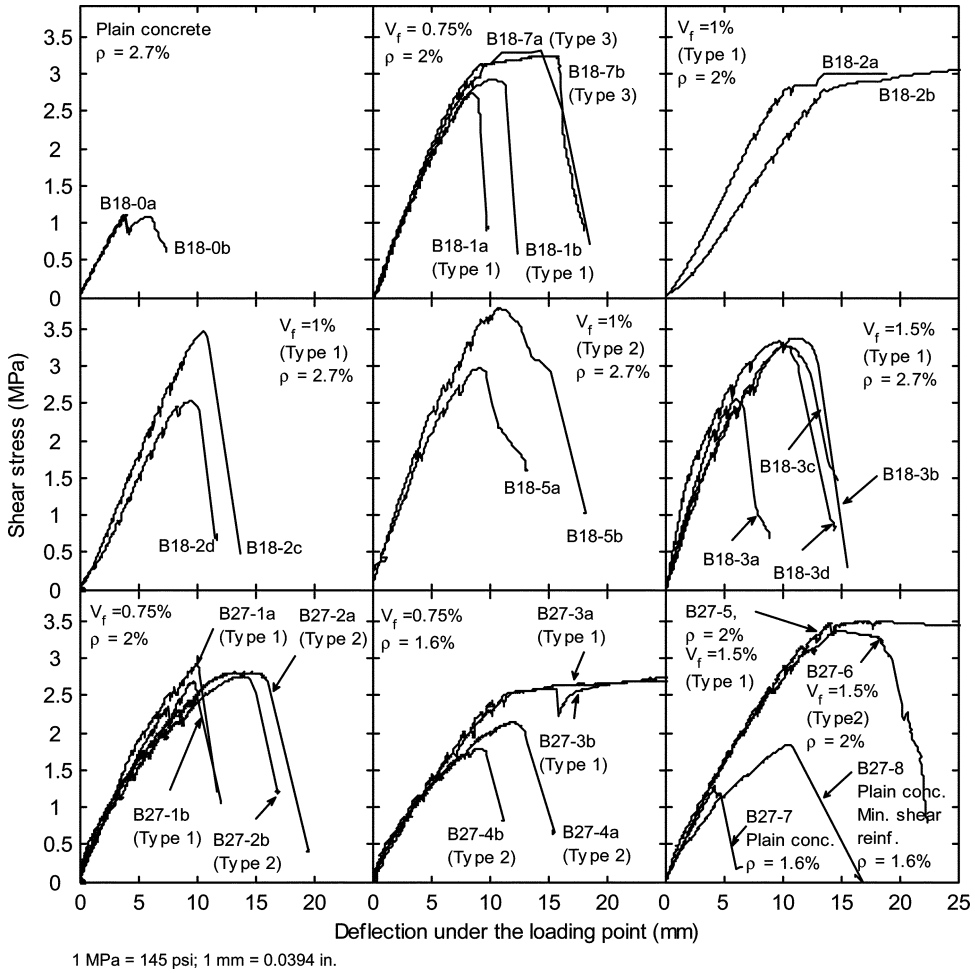

Fig. 6—Average shear stress versus displacement response.

attributed to either voids that developed during concrete casting, lumping of fibers along the longitudinal reinforcement, or a combination of both.

The fact that two different types of shear failures occurred in beams of the same pair is a clear indication of the impossibility of predicting one type of shear failure for a given beam. In some cases, a cracking pattern first developed that indicated the possibility of a shear-compression failure, followed later by the opening of a different diagonal crack that led to a diagonal tension failure. Thus, although a distinction has been made with regard to the type of shear failure exhibited by each beam, it is believed that all types of shear failure should be lumped together when evaluating the overall behavior and shear strength of SFRC beams.

Ultimate strength

The peak (ultimate) average shear stress for each beam is listed in Table 1. As can be seen, the ultimate shear stress for the RC beams was 1.1 and 1.3 MPa (159 and 188 psi) for Series B18 and B27, respectively. These stresses corresponded to $0.17\sqrt{f_c'}$ and $0.21\sqrt{f_c'}$ MPa ($2.0\sqrt{f_c'}$ and $2.5\sqrt{f_c'}$ psi) for Series B18 and B27, respectively. The maximum measured ultimate shear stress for the SFRC beams in these two series was 3.8 MPa (547 psi) (Beam B18-5b) and 3.5 MPa (507 psi) (Beam B27-5), respectively. It is worth mentioning that these maximum shear stresses occurred, as expected, in the beams with the higher fiber volume fractions and larger longitudinal reinforcement ratios. The corresponding normalized ultimate shear stress for these two SFRC beams was $0.54\sqrt{f_c'}$ and $0.53\sqrt{f_c'}$ MPa ($6.5\sqrt{f_c'}$ and $6.3\sqrt{f_c'}$ psi), respectively. This level of normalized shear stress was 3.2 and 2.5 times greater than that in the control specimens of Series B18 and B27, respectively.

The lowest normalized shear strength was exhibited by Beam B27-4b ($0.33\sqrt{f_c'}$ MPa [$4.0\sqrt{f_c'}$ psi]). This shear strength, however, is 10% greater than the lower bound for the shear strength of SFRC beams with at least 0.75% volume fraction of deformed steel fibers reported by Parra-Montesinos (2006). All other SFRC beams tested in this investigation exhibited a normalized shear strength of at least $0.38\sqrt{f_c'}$ MPa ($4.6\sqrt{f_c'}$ psi).

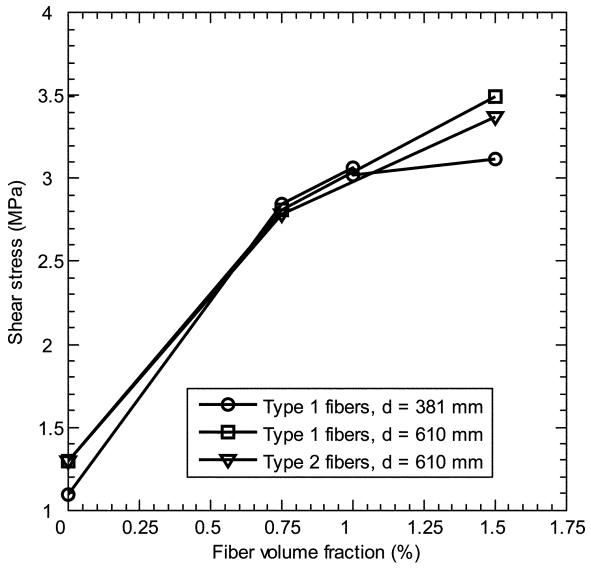

Fig. 7—Average shear stress versus fiber volume fraction. (Note: 1 mm = 0.0394 in.; 1 MPa = 145 psi.)

Effect of fiber volume fraction

The average shear stress versus fiber volume fraction relationship shown in Fig. 7 indicates that an increase in fiber volume fraction resulted in an increase in shear strength, as expected. All SFRC beams shown in Fig. 7 contained a longitudinal reinforcement ratio ρ approximately equal to 2.0%, while ρ was equal to 2.7% and 1.6% in the RC beams (fiber volume fraction = 0 in Fig. 7) with effective depth d of 381 and 610 mm (15 and 24 in.), respectively. The increase in shear strength was significant when fibers were added in a 0.75% volume fraction compared to the beams with no fibers. The efficiency of fiber reinforcement for increasing shear strength, however, seemed to diminish when used in higher volume fractions, particularly beyond 1% by volume.

Effect of fiber type

A comparison of the ultimate shear strengths listed in Table 1 for pairs of SFRC beams constructed with similar effective depth, fiber volume fraction, and longitudinal reinforcement ratio, but with different types of fibers, indicated the following: 1) SFRC beams constructed with Type 3 fibers exhibited only 17% higher normalized shear strength compared to those with Type 1 fibers. It should be kept in mind that the aspect ratio and strength of Type 1 fibers were 2/3 and 48% those of Type 3 fibers, respectively; and 2) the normalized shear strength of the beams with Type 2 fibers, which also had a greater aspect ratio (longer fibers), ranged from 85 to 132% of that of the beams with shorter (Type 1) fibers.

Effect of longitudinal reinforcement ratio

Three longitudinal reinforcement ratios were investigated: 1.6%, approximately 2.0% (1.96% in Series B18 and 2.06% in Series B27), and 2.7%. The effect of longitudinal reinforcement ratio on beam behavior was evaluated by comparing the behavior of nearly "identical" beams with either 1.6 or 2.0% reinforcement ratio, and with 2.0 or 2.7% reinforcement ratio. These changes in flexural reinforcement ratio were not large enough to lead to any significant change in shear strength.

The primary effect of longitudinal reinforcement ratio was on beam ductility. Flexural yielding was observed in several beams with a longitudinal reinforcement ratio of approximately 2.0% (refer to Table 1), whereas no yielding occurred in any of the beams with a 2.7% reinforcement ratio (except for minor yielding in Beam B18-2c). For beams with a 2.0% longitudinal reinforcement ratio, the shear strength of beams with a 0.75% fiber volume fraction, prior to flexural yielding, was believed to be close to the shear demand associated with flexural yielding. Therefore, the occurrence and extent of flexural yielding in these beams was primarily dictated by fiber content. For example, while flexural yielding was not observed in Beam Pairs B27-1 and B27-2 with a 0.75% fiber volume fraction, Beams B27-5 and B27-6, with a 1.5% fiber volume fraction of Type 1 and Type 2 fibers, respectively, exhibited substantial flexural yielding prior to shear failure.

Effect of beam depth

The effect of beam depth on beam shear strength for the range considered was negligible. For example, an increase in total beam depth from 455 to 685 mm (18 to 27 in.) resulted in a slight decrease in shear strength (approximately 7%, on

average) for the beams with Type 1 fibers in a volume fraction of 0.75% and a longitudinal reinforcement ratio of approximately 2.0%. As discussed previously, the increase in beam depth did have an effect on crack spacing, the deeper beams exhibiting wider spacing. When normalized by the effective beam depth, however, the average horizontal crack spacing was approximately the same (on the order of 0.4*d*).

Concrete strain field

The strain growth associated with shear distress was relatively similar in all of the SFRC beams. Figure 8(a) shows a sketch of the cracking pattern at failure for Beam B27-2b, along with the location and numbering of elements used in the infrared tracking system. This beam contained a 0.75% volume fraction of Type 2 fibers and a longitudinal reinforcement ratio of approximately 2.0%. The distribution of vertical (transverse) strains along the critical shear span for various loads, averaged over the beam depth, is shown in Fig. 8(b). Transverse strains started to increase noticeably at loads greater than 623 kN (140 kips) (shear stress of $0.38\sqrt{f'_c}$ MPa [$4.5\sqrt{f'_c}$ psi), due to the formation of diagonal cracks. At 710 kN (160 kips) (shear stress of $0.43\sqrt{f'_c}$ MPa [$5.2\sqrt{f'_c}$ psi]), a substantial increase in transverse strains can be seen due to the formation of what turned out to be the critical diagonal crack

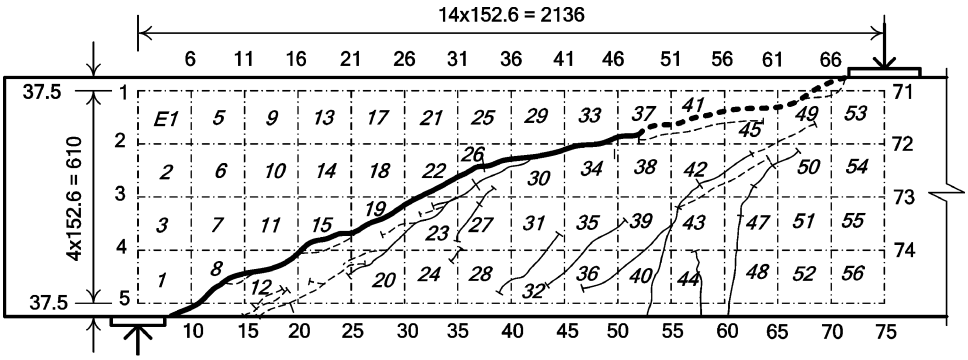

(a) **Element and marker numbering**

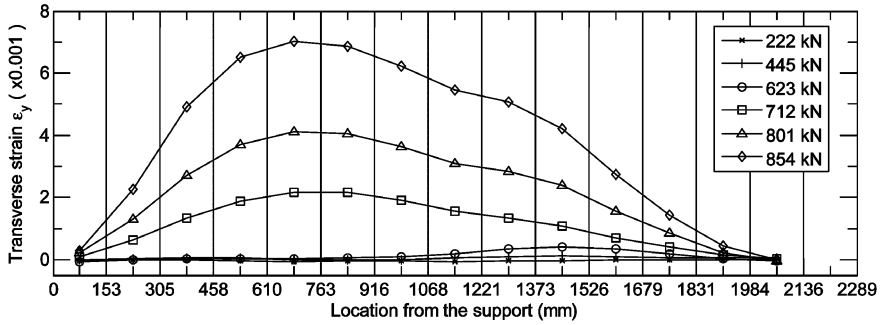

(b) **Vertical strains at various loads, averaged over beam depth**

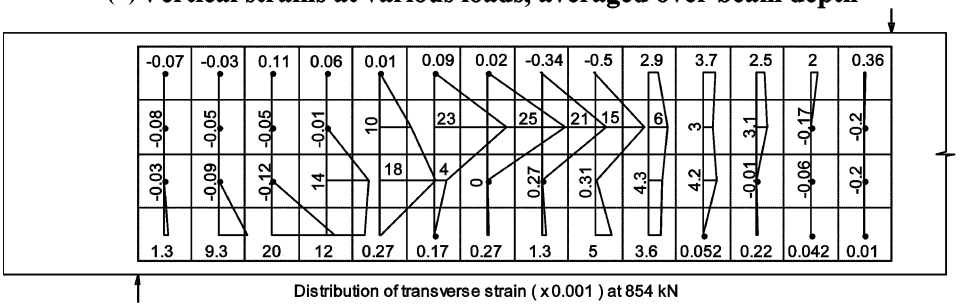

(c) **Distribution of vertical strains at peak load**

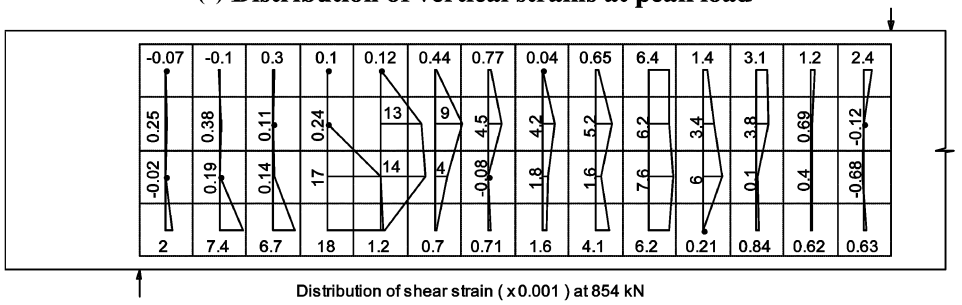

(d) **Distribution of shear strains at peak load**

Fig. 8—Strain distribution for Beam B27-2b. (Note: 1 kN = 0.225 kips; 1 mm = 0.0394 in.)

(Fig. 8(a)). The widening of this crack led to a substantial growth in average transverse strains, which reached a peak of 0.7% prior to shear failure of the beam.

A detailed distribution of vertical (transverse) and shear strains at peak load for Beam 27-2b is provided in Fig. 8(c) and (d), respectively. As can be seen, strain magnitudes were highly sensitive to the location of the cracks, which led to large strains in elements along the main diagonal crack. The maximum transverse and shear strains were 0.025 (Element 26) and 0.018 radians (Element 16), respectively.

For the beams reinforced with shorter (30 mm [1.2 in.] long) fibers, the peak transverse and shear strains at failure were generally smaller compared to those in the beams with longer (60 mm [2.4 in.] long) fibers. This reduction in the magnitude of peak strains was due to the fact that the shorter fibers were less effective in transferring tension across larger

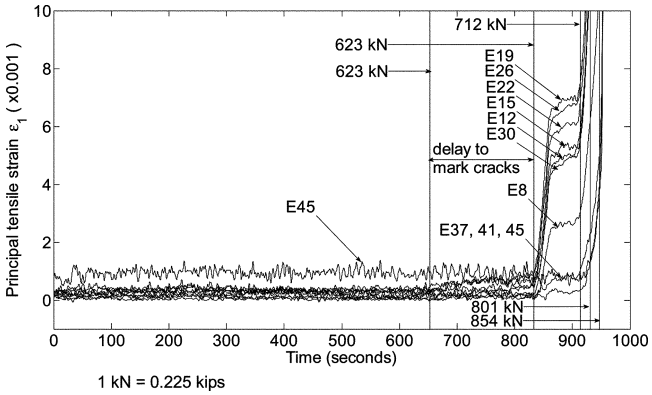

Fig. 9—Development of principal tensile strains in Beam B27-2b.

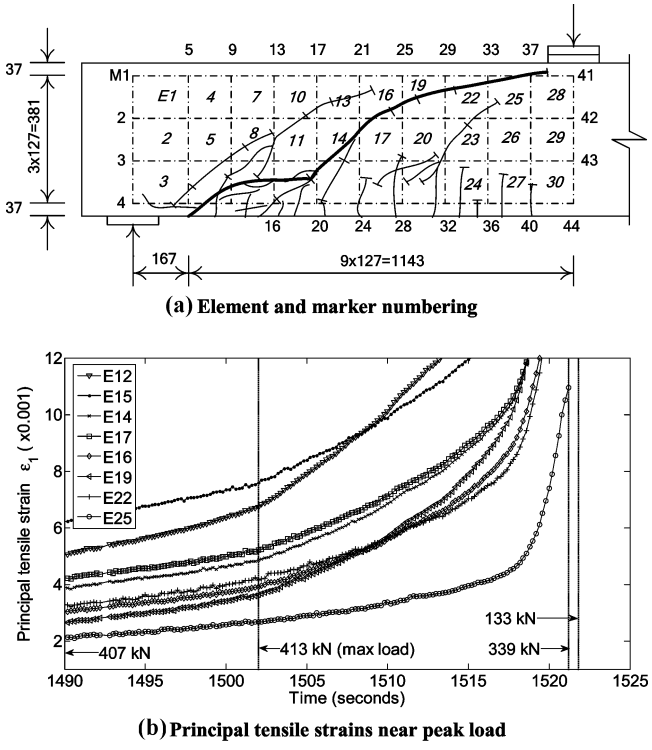

Fig. 10—Development of principal tensile strains near peak load in Beam B18-1b. (Note: 1 kN = 0.225 kips; 1 mm = 0.0394 in.)

crack widths, as evidenced by the results from the ASTM C1609 tests shown in Fig. 4. Thus, a decay in the fiber contribution to shear strength and, thus, shear failure occurred at smaller crack widths (and smaller average vertical and shear strains) for the beams with shorter fibers.

The development of principal tensile strains along the critical crack for Beam 27-2b is shown in Fig. 9. When the applied load exceeded 623 kN (140 kips), significant strains developed for middepth elements (Elements 19, 22, 26, and 30), which then propagated to the reinforcement level (Elements 15, 12, and 8) and compression region (Elements 37, 41, and 45). A significant increase in the straining rate associated with the widening of the critical crack occurred when the beam was loaded beyond 712 kN (160 kips), which ultimately led to failure at a load of 854 kN (192 kips).

In some beams, the opening of the critical diagonal crack started from the bottom of the beam, as opposed to from the beam middepth. An example of such behavior is that exhibited by Beam B18-1b. In this beam, a significant increase in principal tensile strains started at the bottom of one of the diagonal cracks (Fig. 10). From the load of 365 to 413 kN (82 to 93 kips), the rate of increase for principal tensile strains was higher for Element 12. In terms of magnitude, the principal tensile strain decreased from Element 15 to 12, 17, 14, 22, 16, 19, and 25. Beyond the peak load, the principal tensile strain rate and magnitude for these elements increased rapidly, except for Element 25 (beam compression zone near load point), for which the principal tensile strain rate remained relatively constant up to a load slightly below 355 kN (80 kips).

The principal tensile strain development in Beam 18-1b suggests a shifting in shear-resisting mechanisms, from a combined contribution from fibers, aggregate interlock, dowel action, and the beam compression zone to shear resisted primarily by the compression zone, as the beam was deformed beyond the peak load and the critical diagonal crack widened significantly. This observation was further supported by the shear strain history in the beam compression zone. It was only after there was a distinct change in the growth rate of shear strains that complete failure of the beam occurred, indicating that just prior to collapse, the beam compression zone was the main source of shear resistance.

EVALUATION OF ACI CODE PERFORMANCE CRITERIA FOR SFRC

ACI Building Code (ACI Committee 318 2008) Section 5.6.6.2 prescribes the minimum flexural performance criteria for SFRC based on ASTM C1609 four-point bending tests. According to the ACI Code, to consider an SFRC acceptable for shear resistance, the residual strength at midspan deflections of 1/300 and 1/150 of the span length should not be less, respectively, than 90% and 75% of the first peak (cracking) strength. Further, the amount of fibers provided cannot be less than 0.75% by volume.

When comparing the responses shown in Fig. 4 with the minimum flexural performance criteria specified in the 2008 ACI Code (ACI Committee 318 2008), it was found that only the performance of the SFRCs with 60 mm (2.4 in.) long fibers was satisfactory. The fact that the large-scale SFRC beams with shorter fibers showed a behavior similar to that of the beams with longer fibers suggests the need for a reevaluation of the current ACI Code performance criteria used for acceptance of SFRC.

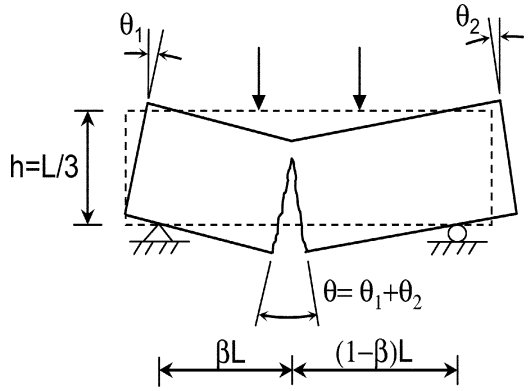

Fig. 11—Assumed rotations in ASTM C1609 beam test.

The similar performance of the large-scale beams with the same fiber volume fraction, regardless of the difference in behavior obtained through ASTM C1609 tests for SFRCs with different fiber lengths, is believed to be due to the substantial difference in maximum diagonal crack width at shear failure between beams with shorter and longer fibers. In the large-scale beams with shorter fibers, these crack widths were substantially smaller than those associated with the maximum deflection applied during the ASTM C1609 beam tests (the former ranging approximately between 25 and 40% of the latter). The maximum crack widths at failure for the beams with longer fibers, on the other hand, were greater and in some cases close to that associated with the maximum deflection of 1/150 of the span length. Failure of the large-scale beams thus initiated at or soon after a diagonal crack width corresponding to that at which a distinct softening of the post-cracking response obtained from the material tests occurred. In general, this crack width represented approximately 5% of the fiber length L_f for both short and long fibers, which suggests that the flexural performance of SFRC could be evaluated based on the residual strength at a deflection limit corresponding to a crack width equal to $0.05L_f$.

The midspan deflection in an ASTM C1609 test corresponding to a crack width of $0.05L_f$ was calculated assuming that, after flexural cracking, the beam behaves as two rigid bodies rotating relative to each other at the crack location (Fig. 11). Defining the shortest distance between the crack section and one of the supports as βL, where β ranges between 1/3 and 1/2 and L is the beam span length, the relative rotation at the crack location θ can be expressed as a function of the beam midspan deflection as follows

$$\theta = \frac{2\delta_{midspan}}{\beta L} \quad (1)$$

Assuming the neutral axis depth at the crack location is equal to 10% of the beam height h, which is reasonable based on test observations, and considering the fact that $h = L/3$, the rotation θ_{max} corresponding to a crack width equal to $0.05L_f$ can be estimated as follows

$$\theta_{max} = \frac{0.05L_f}{0.9h} = \frac{0.05L_f}{0.3L} \quad (2)$$

Combining Eq. (1) and (2) and maximizing the midspan deflection by setting $\beta = 1/2$, the following midspan deflection limit for measuring residual flexural strength is recommended

$$\delta_{midspan} = \frac{L_f}{24} \quad (3)$$

where $L_f \geq 30$ mm (1.2 in.) due to lack of data for beams with shorter fibers.

The deflection limit to be used in an ASTM C1609 beam test with 30 mm (1.2 in.) long fibers would then become 1.25 mm (0.05 in.), whereas that for beams with 60 mm (2.4 in.) long fibers would be 2.5 mm (0.1 in.). If the current ACI Code residual strength factor of 0.75 is used at the proposed midspan deflection limit in Eq. (3) rather than at 1/150 of the span length, the performance of the SFRC material with short, high-strength fibers (Type 3) would be satisfactory, whereas that of the SFRC with short, regular-strength fibers (Type 1), even though it is close to the limit, would still be inadequate. This suggests the need for a relaxation of the residual strength factor limits, but additional experimental data are required to justify such a change.

A second strength limit of 40% of the first peak load at a deflection of 1/150 of the span length is proposed to prevent the use of an SFRC material with an unacceptably low residual strength at larger crack widths.

CONCLUSIONS

The following conclusions can be drawn from the results of this experimental investigation.

- The use of hooked steel fibers in a volume fraction greater than or equal to 0.75% led to an enhanced inclined cracking pattern (multiple cracks) and improved shear strength in beams without stirrup reinforcement, greater than or equal to $0.33\sqrt{f'_c}$ MPa ($4.0\sqrt{f'_c}$ psi). The increase in shear strength associated with an increase in fiber content beyond 1% by volume, however, was relatively small.
- A comparison of the behavior of the SFRC beams with that of the RC beam with stirrup reinforcement satisfying the minimum requirement in the 2008 ACI Code indicates that any of the three types of hooked steel fibers evaluated in this investigation, when used in a volume fraction greater than or equal to 0.75%, can be used in place of the minimum stirrup reinforcement required by ACI Committee 318.
- Hooked steel fibers with a length of 60 mm (2.4 in.) allowed a greater inclined crack opening before failure compared to that observed in beams with 30 mm (1.2 in.) long fibers, but they were prone to problems associated with fiber lumping along the longitudinal reinforcement. A horizontal clear spacing between reinforcing bars no less than the fiber length is therefore recommended.
- The difference in diagonal crack width at shear failure for beams with short (30 mm [1.2 in.] long) versus long (60 mm [2.4 in.] long) fibers indicates that the use of a deflection limit that is a function of fiber length should be used for evaluating the flexural performance of SFRC based on ASTM C1609 tests, as opposed to fixed limits that are a function of the beam span length. Based on test results, a target crack width equal to 5% of the fiber length L_f was found to be adequate, which led to the proposed deflection limit of $L_f/24$. Until further data become available, residual

strength limits of 75% and 40% of the first peak load are recommended for use at beam midspan deflections equal to $L_f/24$ and 1/150 of the span length, respectively.

ACKNOWLEDGMENTS

The authors would like to acknowledge the support of Bekaert Corporation, which donated the hooked steel fibers used in this investigation.

REFERENCES

ACI Committee 318, 2008, "Building Code Requirements for Structural Concrete (ACI 318-08) and Commentary," American Concrete Institute, Farmington Hills, MI, 473 pp.

ASTM C1609/C1609M-05, 2005, "Standard Test Method for Flexural Performance of Fiber-Reinforced Concrete (Using Beam With Third-Point Loading)," ASTM International, West Conshohocken, PA, 9 pp.

Dinh, H. H., 2009, "Shear Behavior of Steel Fiber Reinforced Concrete Beams without Stirrup Reinforcement," doctoral dissertation, Department of Civil and Environmental Engineering, University of Michigan, Ann Arbor, MI, 285 pp.

Northern Digital Inc., 2005, "NDI OptoTRAK Certus User Guide," Waterloo, ON, Canada.

Parra-Montesinos, G. J., 2006, "Shear Strength of Beams with Deformed Steel Fibers," *Concrete International*, V. 28, No. 11, Nov., pp. 57-66.

Wight, J. K., and MacGregor, J. G., 2008, *Reinforced Concrete: Mechanics and Design*, fifth edition, Pearson Prentice Hall, Upper Saddle River, NJ, pp. 247-248.